ELECTRO- AND MAGNETOBIOLOGY, 20(3), 371–396 (2001)

Electromagn Biol Med Downloaded from informahealthcare.com by CDL-UC San Diego on 06/03/15
For personal use only.

ELECTROMAGNETIC ACTIVITY OF YEAST CELLS IN THE M PHASE

J. Pokorný,[1,*] J. Hašek,[2] F. Jelínek,[1] J. Šaroch,[1] and B. Palán[3]

[1]Institute of Radio Engineering and Electronics, Academy of Sciences of the Czech Republic, Chaberská 57, 182 51 Prague 8, Czech Republic
[2]Institute of Microbiology, Academy of Sciences of the Czech Republic, Vídeňská 1083, Prague 4, Czech Republic
[3]Faculty of Electrical Engineering, Czech Technical University, Technická 2, Prague 6, Czech Republic

ABSTRACT

Electromagnetic activity around yeast mitotic cells (*Saccharomyces cerevisiae*) was measured in the frequency range 8–9 MHz and special care was taken to extract reliable information from the raw signals. The characteristic of cold-sensitive tubulin mutants *tub2-401* and *tub2-406*, which come to arrest before mitosis at a restrictive temperature (14°C) and which re-enter mitosis upon a shift back to a permissive temperature (28°C), was used to prepare synchronized mitotic cells. Immunofluorescence microscopy using an anti-tubulin antibody was used to analyze microtubular structures. The arrested *tub2-401* mutant that had back-shifted to permissive temperature displayed no microtubules and no electromagnetic activity around the cells. In contrast, the arrested cells of the mutant *tub2-406* displayed developed, but aberrant, nonfunctional microtubules and a high electromagnetic activity around the cells. The electromagnetic activity around the arrested mutant *tub2-401* back-shifted to permissive temperature peaks at four time points which may coincide with (i) formation of the mitotic spindle, (ii) binding of chromatids to kinetochore microtubules, (iii) elongation of the spindle in anaphase A, and (iv) elongation of the spindle in anaphase B. The profile of the electromagnetic

* Corresponding author. Fax: 420 2 688 0222; E-mail: pokorny@ure.cas.cz

Copyright © 2001 by Marcel Dekker, Inc. www.dekker.com

RIGHTSLINK

ORDER REPRINTS

activity around the synchronized mutant *tub2-406* at permissive temperature seems to be delayed by the time required for aberrant nonfunctional microtubules to be depolymerized. Experimental results presented in this paper support Pohl's idea of existence of the electromagnetic field around yeast cells.

Key Words: M phase; Microtubule electromagnetic activity; *Saccharomyces cerevisiae*

Electromagn Biol Med Downloaded from informahealthcare.com by CDL-UC San Diego on 06/03/15
For personal use only.

INTRODUCTION

Mechanisms that regulate order in biological systems are largely unknown. We do not know, e.g., how the energy of ATP hydrolysis couples to protein to create physical force. Because biological matter has extraordinary polar and polarization properties, the ordering mechanisms are assumed to be electromagnetic in nature. Frauenfelder et al. discussed the nature of forces between biomolecules, organelles, and living cells, with the conclusion that ''in biological physics, the force is known, it is the electromagnetic interaction'' (1). Because of ubiquitous thermal vibrations, polarization waves exist in any polar system, and an electromagnetic field with a dominant electrical component is generated in its vicinity. Fröhlich assumed that energy supplied to polarized biological structures condenses in one vibration mode due to nonlinear energy exchange with the surroundings (2–5). A similar mechanism of energy condensation may depend on internal nonlinear properties of the oscillation system (6). Microtubules and actin filaments in the cytoskeleton are the structures with an energy supply that meet the requirements of Fröhlich coherent vibrations (7). Nevertheless, experimental verification of the Fröhlich hypothesis is still lacking.

The assumption that electromagnetic forces have a fundamental role in the mechanisms of organization of living matter is supported by indirect as well as direct measurements of the electromagnetic field around living cells. Pohl observed the attraction of small dielectric particles to cells (8,9). He explained these results as dielectrophoretic effects—the inhomogeneous electromagnetic field attracts particles whose permitivity is greater than that of the ambient medium in a region with a greater electric field, i.e., toward the plasma membrane. The greater the permitivity of the particles, and the smaller the conductivity of the suspension of cells, the greater the number of attracted particles. In the M phase of the cell cycle, yeast cells attract the greatest number of particles. In the M phase, microtubules form a mitotic spindle which has a dominant role in the cell. Microtubules are polar and accept large amounts of energy from the hydrolysis of guanosine triphosphate (GTP) (through the mechanism of dynamic instability and treadmilling) (10–12). It is well known that microtubules in the cytoskeleton exert forces and generate movements without any major chemical changes.

Rowlands observed interactions between red blood cells and formation of rouleaus (13). The interaction forces act between the red blood cells up to a distance of about 1 μm. Albrecht-Buehler described the ability of cells to detect electromagnetic signals of other cells in the red or near-infrared range (14). Vos et

Copyright © Marcel Dekker, Inc. All rights reserved.

MARCEL DEKKER, INC.
270 Madison Avenue, New York, New York 10016

RIGHTSLINK

ORDER REPRINTS

al. (15) measured stimulated emission from membrane proteins of photosynthetic bacteria *Rhodobacter capsulatus* in the near-infrared region. Coherent spectral lines were measured at 15 cm^{-1} (450 GHz) and 77 cm^{-1} (2.3 THz).

Indirect measurements are based on the force effects of the electromagnetic fields. Forces of various origins can participate in the final effect. Because of the hypothetical role of the electromagnetic field in organization of living matter, direct measurements of the electromagnetic field generated by living cells are of the utmost importance. Direct measurements of the electromagnetic field generated by yeast cells are described in references 16–19. Clusters of synchronized yeast cells in the M phase sealed together by an electric field were measured by Smith (16). Hölzel and Lamprecht (17) measured yeast cells in the frequency band of about 1–100 MHz using platinum electrodes on a glass substrate (microscope slide) as a detector, a high-impedance preamplifier, and a spectrum analyzer. ''Cells were dielectrophoretically collected in the gap between electrodes in such a way that their ends were in contact with each electrode'' (17). The spectral lines which exceeded the value corresponding to a probability of 99.9% for not being of noise origin were accepted as signals.

We used a similar measurement system and measured synchronized cultures of *Saccharomyces cerevisiae* in the M phase of the cell cycle (19). The electromagnetic field decreases steeply with increasing distance from the plasma membrane, as follows from theoretical analysis (6), and the intensity of the electric field has to be measured within a distance of 0.1 μm. Therefore, only special sensors can detect the intensity of the electric field in the vicinity of the plasma membrane. We used sensors with electrodes evaporated on glass (19). The measured power of the cellular field was of the order of 10^{-16}–10^{-17} W (19). The experimental results in reference 19 suggested that the electromagnetic activity peaked at the time corresponding to the beginning of metaphase (when the kinetochore microtubules in the mitotic spindle bind chromatids) and when the majority of cells proceed into anaphase B. Suspending liquid without cells was used for control experiments. Further experimental investigations of the electromagnetic fields of cells are necessary to verify experimental conditions of the measurement (e.g., dependence on the detector structure, on the other experimental facilities, and on the control experiments), to find more detailed characteristics of the field, and to analyze the time dependence of the measured electromagnetic field.

MATERIALS AND METHODS

Cultivation of Cells

Cold-sensitive β-tubulin mutants *tub2-401* [strain CUY67 Mata *tub2-401 ura3-52 ade2-101* (20)] and *tub2-406* [strain CUY393 Mata *tub2-406 ura3-52 his4* (20)] of *S. cerevisiae* were cultivated in YPD medium (2% glucose, 2% peptone, 1% yeast extract) at 28°C for 16 hr (21). Cells from the exponential phase were transferred to fresh YPD medium and further cultivated at restrictive temper-

Electromagn Biol Med Downloaded from informahealthcare.com by CDL-UC San Diego on 06/03/15
For personal use only.

Copyright © Marcel Dekker, Inc. All rights reserved.

MARCEL DEKKER, INC.
270 Madison Avenue, New York, New York 10016

RIGHTSLINK

ORDER REPRINTS

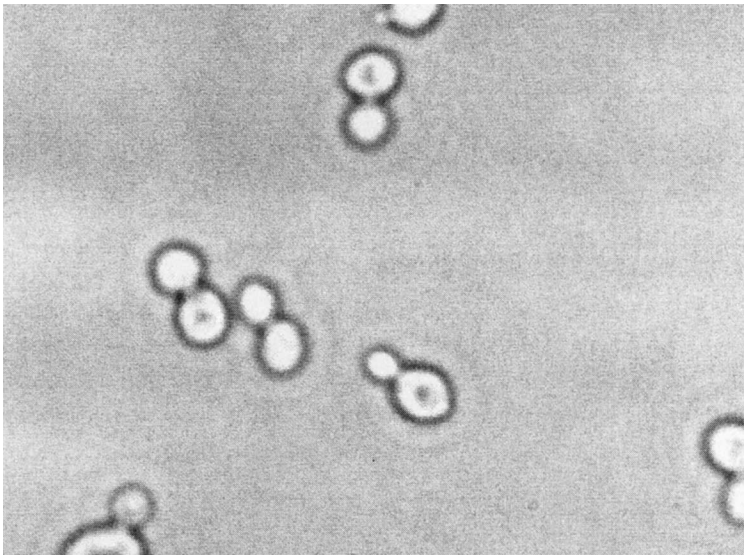


Figure 1. Tubulin mutant *tub2-401* of yeast cells *Saccharomyces cerevisiae* before measurement.

ature (14°C) for 4 hr. Before measurements, the cells were washed three times with cold (14°C) deionized 0.06 M sucrose. To start experiments, the suspension of arrested cells (OD 600 app. 4.5) in 0.06 M sucrose was warmed to permissive temperature (≥28°C). In experiment groups 1, 2, 3, and 4 the OD 600 value was in the range from 1 to 2.5 and in group 5, the density was in the range 4–5. Concentration of cells of the mutant *tub2-406* corresponding to OD 600 4.5 is about 2×10^8 cells/ml. In the arrested population before mitosis we found approximately 85–90% enlarged budded cells. Cells of the mutant *tub2-401* after warming to the permissive temperature are shown in Figure 1.

The nonsynchronized wild type cells [strain CUY8 Matα *ade2-101 ura3-52* (20)] used in control experiments were prepared in a similar way as the mutant cells.

Immunofluorescence Microscopy

To document the phase of the mutant cell recovery from the mitotic arrest, the cells resuspended in cold 0.06 M sucrose were analyzed by immunofluorescence microscopy at various time points after warming to the permissive temperature. Cells in sucrose were fixed with 3.7% formaldehyde for 2 hr and processed for immunolabeling as described by Hašek and Streiblová (21). Rabbit polyclonal antibody 206-1 against the C-terminal domain of the yeast β-tubulin (kindly provided by Dr. F. Solomon from MIT) was used to visualize microtubules. As a secondary antibody, goat anti-rabbit immunoglobulin (IgG) antibody conjugated with CY3 fluorescent dye (Sigma-Aldrich, St. Louis, MO) was applied.

Electromagn Biol Med Downloaded from informahealthcare.com by CDL-UC San Diego on 06/03/15
For personal use only.

Copyright © Marcel Dekker, Inc. All rights reserved.

Marcel Dekker, Inc.
270 Madison Avenue, New York, New York 10016

RIGHTSLINK

ORDER REPRINTS

Detection Electrodes

Sensors are the key part of the measurement system. Sensors must detect the electric component of the electromagnetic field in the very near vicinity of the cells (no field can be measured at a distance greater than about 0.1 μm from the cell). This is an important requirement of the design. Two types of sensors were designed and prepared during development of the measurement method. The first consists of metal strips on glass and alumina substrates [this type is similar to sensors used by Hölzel and Lamprecht (17)]. The second type consists of a microelectronic configuration of electrodes deposited on a silicon substrate.

The preparation of the first type was done in a high vacuum (2.6×10^{-5} Pa). Pairs of metal strips 400 μm wide with a composition of 30 nm Ti/200 nm Au were evaporated onto glass or alumina substrates through a metal mask. The strips were broadened at the ends to form contacting pads. Then an insulating layer of SiO_2 was evaporated onto the surface with the electrodes. At places where measured living cells should be inserted, 8-μm-wide gaps in the layer were formed by etching. Finally, to improve the electrical interruption of the strip electrodes in the gap, a spark discharge was applied. Thus, a miniature cuvette was formed on the glass or alumina plate. The sensors are schematically shown in Figure 2.

The second type, the microelectronic sensor, is a chip using complementary metal-oxide semiconductor (CMOS) technology. Seven pairs of metal strips were formed on a silicon substrate with dimensions of 5 mm × 5 mm, covered by an

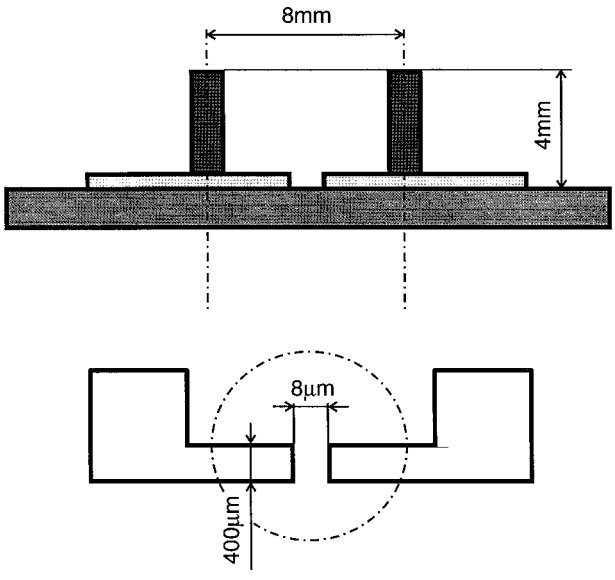


Figure 2. Schematic illustration of a sensor with two gold strips evaporated on an alumina substrate. After reference 19.

Electromagn Biol Med Downloaded from informahealthcare.com by CDL-UC San Diego on 06/03/15
For personal use only.

Copyright © Marcel Dekker, Inc. All rights reserved.

MARCEL DEKKER, INC.
270 Madison Avenue, New York, New York 10016

RIGHTSLINK

ORDER REPRINTS

insulating SiO_2 layer 3 μm thick. The widths of strips were about 10 μm and the gap between strips in a pair increased from pair to pair from 2 μm to greater widths in sequence. The electrodes were covered by a chemical vapor deposited SiO_2 layer. A square window was etched only above the gap between electrodes. This window was intended for inserting cells. The layout of the sensor chip is shown in Figure 3. Dimensions of the contact electrodes and windows are given in reference 19. A photomicrograph of one pair of strips digitally processed is shown in Figure 4. The whole sensor is shown in Figure 5.

Measurement System

A block diagram of the measurement system for detection of electromagnetic oscillations of living cells is shown in Figure 6 for the Rohde & Schwarz FSEA30 (R&S) spectrum analyzer. The block diagram for measurement with the Anritsu MS710F (ANR) spectrum analyzer is different—a printer is connected to the output of the spectrum analyzer instead of a computer. The sensor, together with the following preamplifier, were placed in a doubly shielded box. An outer mumetal screening box (from the Czech Research Institute of Metals) for magnetic and electrical fields (thickness of the sheet is about 0.5 mm) and an inner box for additional electrical and light screening were used. Each box was grounded at one point by connecting it to the outer tube of the output coaxial line.

The effectiveness of the screening was measured using a signal generator with an output power of 0.5 W. Near zone electric or magnetic fields were generated around the shielding boxes. We measured the output signal of the spectrum analyzer when the upper covers of both boxes were removed, when the cover of one of them was removed, and when both the boxes had upper covers. Even if both the upper covers were removed, the system was partially screened by the remaining parts of the boxes. In this case the spectral line at the frequency of the generator was about 65–70 dB above the mean value of the noise. If at least one of the boxes had the upper cover, no output signal was registered even after integration for about 10 min.

The input circuit connected the sensor to the first stage of the preamplifier. Noise originated from electrolysis at the electrodes was avoided by using a capacitor in series with the input (the capacitor separated the DC current of the input of the preamplifier from the sensor). A resistor of 0.5 MΩ was connected in parallel to the input of the preamplifier.

The first stage of the preamplifier used an integrated amplifier MAX4005. This is a ''unity gain buffer with a high-impedance JFET'' (junction field effect transistor) input which drives a 75 Ω load. Voltage gain was about 0.5 and input resistance and capacitance were >1 MΩ and 2 pF, respectively. The second stage used a low-noise operational amplifier AD640JN. The power supply of the preamplifier was provided by batteries, which were placed in a doubly shielded box.

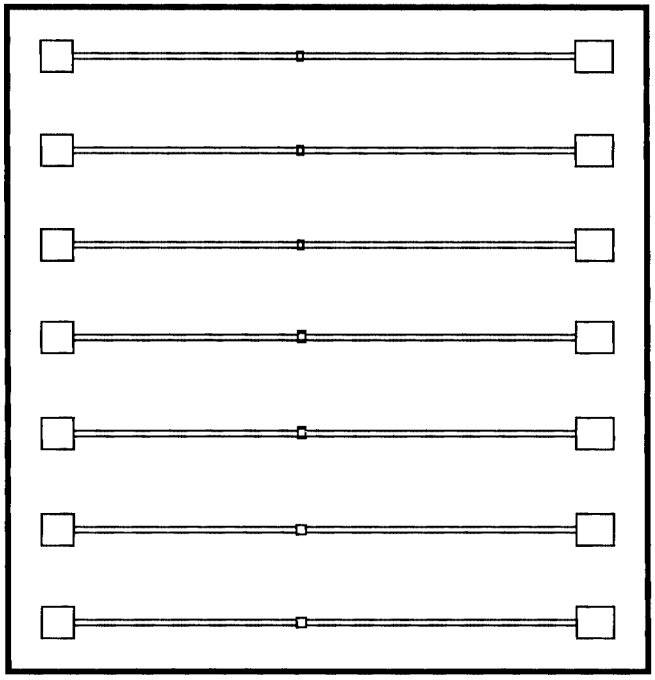
Electromagn Biol Med Downloaded from informahealthcare.com by CDL-UC San Diego on 06/03/15
For personal use only.

Copyright © Marcel Dekker, Inc. All rights reserved.

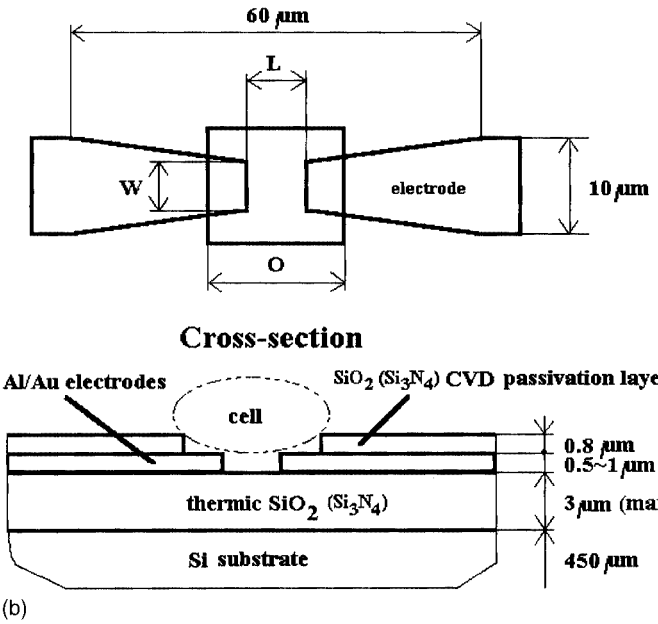
Marcel Dekker, Inc.
270 Madison Avenue, New York, New York 10016

RIGHTSLINK

ORDER REPRINTS



(a)



(b)

Figure 3. A schematic illustration of the microelectronic sensor. The layout of metal strips on the chip (5 × 5 mm) (a) and detail of one electrode pair and the vertical cross-section of the layered structure (b). After reference 19.

Electromagn Biol Med Downloaded from informahealthcare.com by CDL-UC San Diego on 06/03/15
For personal use only.

Copyright © Marcel Dekker, Inc. All rights reserved.

MARCEL DEKKER, INC.
270 Madison Avenue, New York, New York 10016

RIGHTSLINK

ORDER REPRINTS

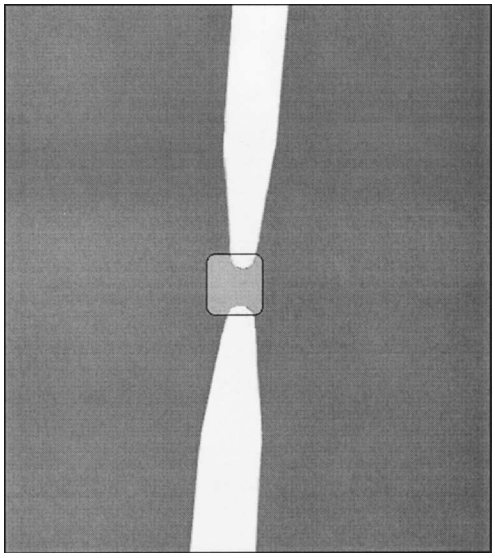


Figure 4. Microscopic image of a microelectronic sensor with two metal strips on a silicon substrate. The widths of strips are about 10 µm and the gap between strips is about 6 µm. After reference 19.

The preamplifier was connected to a spectrum analyzer by a semirigid coaxial cable or by a conventional coaxial cable. We used ANR and R&S spectrum analyzers. The scanning time in the frequency range 8–9 MHz was 100 sec (ANR) or 60 sec (R&S). The resolution and the video bandwith was 300 Hz. The output signal of the spectrum analyzer ANR was observed on the display and recorded in graphic form by a printer. The output signal from the spectrum analyzer R&S

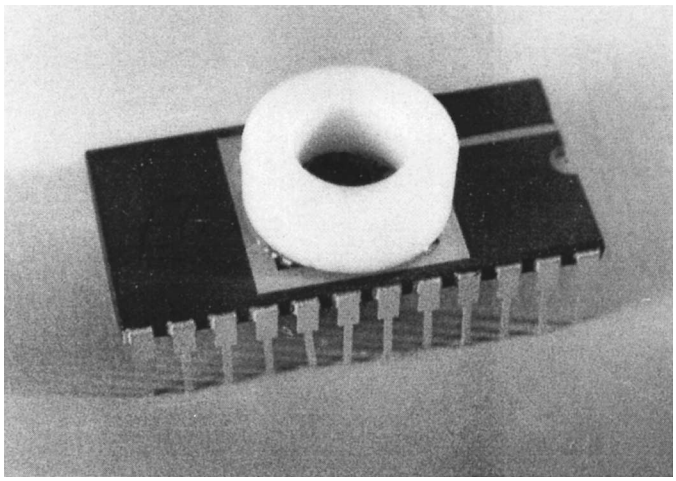


Figure 5. Microelectronic sensor for measurement of yeast cells. The silicon chip with seven pairs of electrodes is at the bottom of the circular cuvette.

Electromagn Biol Med Downloaded from informahealthcare.com by CDL-UC San Diego on 06/03/15
For personal use only.

Copyright © Marcel Dekker, Inc. All rights reserved.

Marcel Dekker, Inc.
270 Madison Avenue, New York, New York 10016

RIGHTSLINK

ORDER REPRINTS

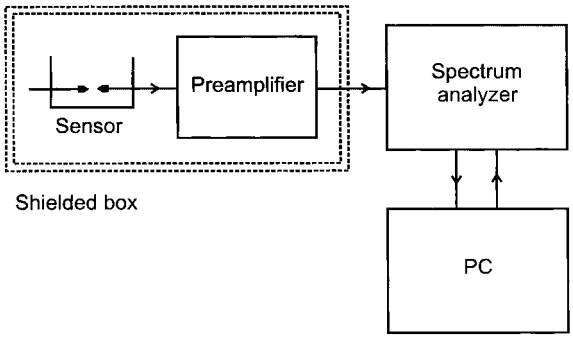


Figure 6. A block diagram of the measurement system. Sensor, preamplifier, and batteries are in the doubly shielded box. The computer (PC) controls the measurement system and stores the output data.

was observed on the display, stored in the memory of a computer (which controls the spectrum analyzer), and evaluated by specially designed computer programs.

Measurement Method

A cell culture in deionized 0.06 sucrose was warmed in a water bath at 33°C for 3 min and then a given volume of the suspension (depending on the sensor but the same volume in one group of experiments) was put in the cuvette of the sensor. The substrate with the electrodes was at the bottom of the cuvette. The cells sedimented in several layers, and coated the bottom of the cuvette. We did not use dielectrophoretic concentration of cells in the gap between electrodes. The cells were randomly oriented. Parallel leakage of the measured signal between electrodes 400 μm wide could decrease signal amplitude. In the gap between electrodes 10 μm wide (in the microelectric sensor), where only one or two cells may be placed, signal amplitude might be greater.

The ambient temperature during measurement was 27 ± 2°C. The beginning of warming in the water bath is the initial time ($t = 0$) for each experiment. The transition from the restrictive to the permissive temperature was delayed with respect to the initial time. We measured over a time interval of 60 or 70 min. The control measurements were carried out with an empty sensor, with pure 0.06 M sucrose solution, and with nonsynchronized yeast cells under the same conditions as the synchronized yeast cells. The number of experiments in particular groups was denoted by N with a corresponding index.

Evaluation of Data

First, we note that the output signal of the preamplifier was a nonlinear function of the input signal, of the noise in the input circuit, and of the noise of the

Electromagn Biol Med Downloaded from informahealthcare.com by CDL-UC San Diego on 06/03/15
For personal use only.

Copyright © Marcel Dekker, Inc. All rights reserved.

Marcel Dekker, Inc.
270 Madison Avenue, New York, New York 10016

RIGHTSLINK

ORDER REPRINTS

preamplifier, dependent on its nonlinear amplification characteristic. We evaluated output data stored in the computer memory (for each measurement the number of values was greater than 1.5×10^5). As a basis for statistical evaluation we used a method similar to that of Hölzel and Lamprecht (17). They considered a spectral line as a signal if its amplitude exceeded a level corresponding to a high value of probability (P_{th}) that the line was not noise. We took for evaluation spectral lines whose amplitudes were about 7–8 and 6 dB above the mean value of the noise in measurements with spectrum analyzer ANR and R&S, respectively. The 6 dB value corresponds to a probability P_{th} of about 0.9995 for the Gaussian distribution of noise. To exclude the influence of systematic error and of noise (a probability of occurence of a noise spectral line is about 0.0005), control measurements were carried out in a standard uniform way. The following evaluation method was used: After dividing the whole time interval of measurement into 5-min subintervals, we summed the number of evaluated spectral lines in the subintervals for each synchronized cell suspension and for control measurements. Then mean values P_Y, P_D, P_C, and P_W were determined in the subintervals for the synchronized cell suspension, for the empty sensor, for the sucrose solution, and for the nonsynchronized cell suspension, respectively. The differences $P_Y - P_D$, $P_Y - P_C$, and $P_Y - P_W$ represent net contributions of synchronized cells to the measured signal.

Mean values of P_Y, P_D, P_C, and P_W were tested using an F-test and a two-group t-test (one sided). Analysis of variance with repeated measures was used to verify hypotheses (i) that there is no difference in the examined parameter (i.e., of the mean value of the number of spectral lines in the subintervals) for synchronized cell and control measurements—H1; (ii) that there is no difference in the magnitude of the parameter in different time subintervals—H2; and (iii) that in the time interval of the measurements, the time course of the parameter does not differ for synchronized cells and control measurements—H3.

RESULTS

Reassembly of Microtubules

Development of microtubule structures in the mutant *tub2-401* of *S. cerevisiae* released from the restrictive to the permissive temperature is shown in Figure 7a (19). Evaluation was done from the fluorescent micrographs representing distribution of β-tubulin molecules stained with antibodies. At the initial time ($t = 0$) when the cells were at the boundary between the G2 and the M phase, spherical nuclei with two spindle pole bodies were visible. Such a stain pattern was typical for more than 98% of cells in the population.

After 20 min of recovery of the arrested mutant at the permissive temperature, the nuclei were elongated and displayed a complete mitotic spindle. Short spindles appeared in more than 96% of cells. After 40 min of cultivation the majority of the cells were in anaphase A (mitotic spindles of these cells were

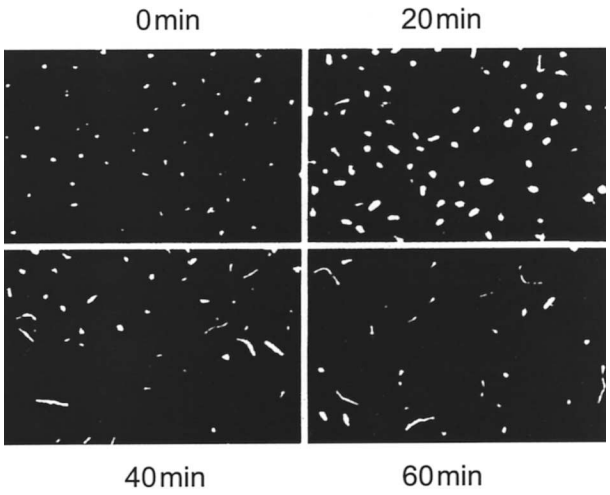
Electromagn Biol Med Downloaded from informahealthcare.com by CDL-UC San Diego on 06/03/15
For personal use only.

Copyright © Marcel Dekker, Inc. All rights reserved.

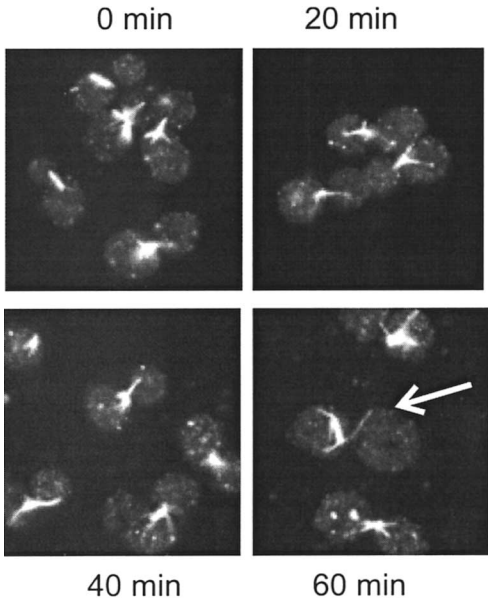
MARCEL DEKKER, INC.
270 Madison Avenue, New York, New York 10016

RIGHTSLINK

ORDER REPRINTS



(a)



(b)

Figure 7. Distribution of β-tubulin revealed by immunofluorescence microscopy with antibody 206-1 (white) in recovering *tub2-401* (after reference 19) (a) and *tub2-406* (b) mutants of *S. cerevisiae*. Measured in time $t = 0$ min, $t = 20$ min, $t = 40$ min, and $t = 60$ min after the shift from a restrictive to a permissive temperature. In (b), the arrow indicates a complete mitotic spindle in $t = 60$ min.

Electromagn Biol Med Downloaded from informahealthcare.com by CDL-UC San Diego on 06/03/15
For personal use only.

Copyright © Marcel Dekker, Inc. All rights reserved.

MARCEL DEKKER, INC.
270 Madison Avenue, New York, New York 10016

RIGHTSLINK

ORDER REPRINTS

elongated) and some of them were in anaphase B (their mitotic spindles were very much elongated). Medium spindles (anaphase A) were observed in 85% of the cells, 10% displayed short spindles, and 5% showed elongated spindles (anaphase B). Within 60 min of cultivation, the mitotic spindles of the majority of cells were very much elongated (anaphase B) and some cells completed anaphase B. Elongated spindles were shown in 70% of cells; 25% of cells displayed medium spindles, and 5% showed G1-specific organization of microtubules. Development of the mitotic spindle in the M phase is schematically shown in the upper parts of Figs. 10–12.

Development of microtubule structures in the arrested mutant *tub2-406* of *S. cerevisiae* shifted back from the restrictive to the permissive temperature is shown in Fig. 7b.

Electromagnetic Activity of Yeast Cells

The output signal measured with the spectrum analyzer R&S and reproduced from the computer memory is shown in Fig. 8. The spectral line at the frequency 8.085 MHz was about 7 dB above the mean value of the noise. The scale on the left-hand side vertical axis shows the input power $P_{R\&S}$ (in dBm) of the spectrum analyzer. The corresponding values of the input power P_{am} (in dBm) of the preamplifier found by calibration using the tracking generator and attenuators are on the right-hand side vertical axis. Input power of the spectrum analyzer R&S (i.e.,

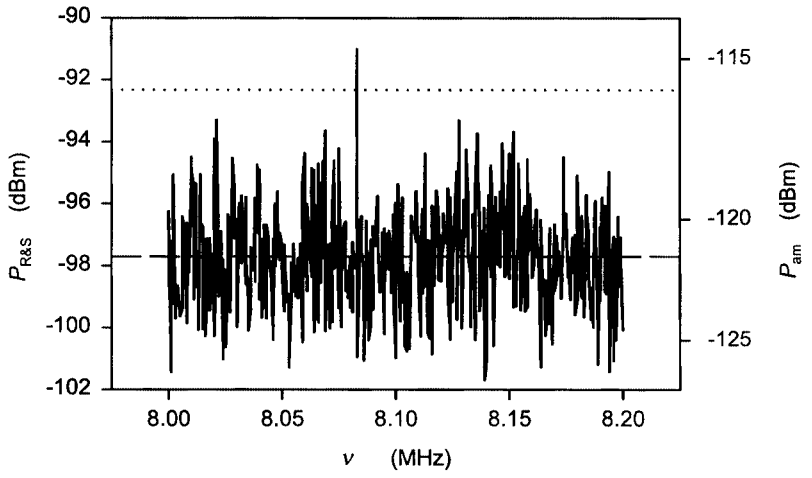


Figure 8. Output signal of the spectrum analyzer R&S as a function of frequency (reproduced from data stored in the computer memory). The dashed line indicates the average value of the noise. The dotted line indicates the critical level for evaluation. The spectral line that exceeds the critical level is about 7 dB above the average value of the noise. The scale on the left-hand side vertical axis denotes input power $P_{R\&S}$ of the spectrum analyser. The scale on the right-hand side denotes input power P_{am} of the preamplifier (with a 50 Ω resistor in the input circuit).

Electromagn Biol Med Downloaded from informahealthcare.com by CDL-UC San Diego on 06/03/15
For personal use only.

Copyright © Marcel Dekker, Inc. All rights reserved.

Marcel Dekker, Inc.
270 Madison Avenue, New York, New York 10016

RIGHTSLINK

ORDER REPRINTS

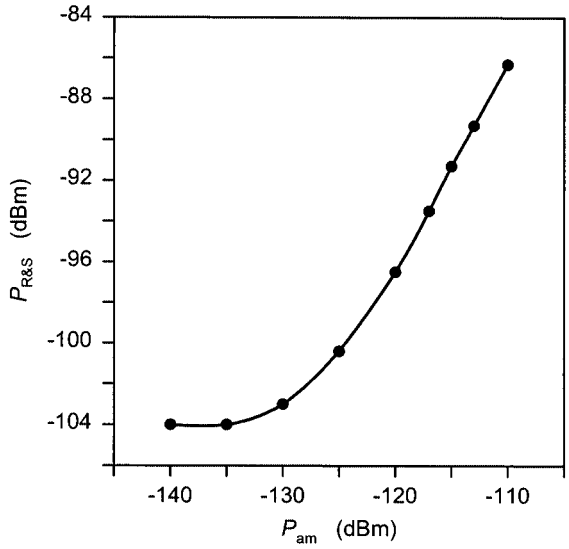


Figure 9. Input power $P_{R\&S}$ of the spectrum analyzer versus input power P_{am} of the preamplifier. Measured with a tracking generator and with a 50 Ω resistor in the input circuit of the preamplifier.

the output power of the preamplifier) versus input power of the preamplifier is shown in Fig. 9. A resistor of 50 Ω was connected instead of the sensor for measurement of the input power, and the input impedance had resistive character. Therefore, the scale on the right-hand side of the vertical axis in Fig. 8 was valid only for this input impedance. The input impedance of the preamplifier was considerably greater than 50 Ω. A resistor of 0.5 MΩ was connected in parallel with the high-input resistance of the ''unity gain buffer'' MAX4005. On the other hand, the capacitance in the input circuit considerably decreased the input impedance. For the parallel capacitance of the input circuit, 1 pF and input capacitance of 2 pF of MAX4005, the input impedance had a capacitive character with an absolute value of about 6–7 $\times$ 10^3 Ω. The real input power (at the same input voltage) was about 20–25 dB lower than the values on the right-hand axis in Fig. 8 (23 dB was used for determination of the noise value). The noise value of the system was about 4 dB. Noise power was evaluated from the measured output noise by integration, and recalculated to the input, taking into account the real input impedance of the preamplifier.

The measured spectral lines had a transient character. We wanted to observe the shape of the spectral lines. When the frequency span was narrowed (the necessary time for accomplishing this is about 20–30 sec), we did not observe the spectral line or we observed a spectral line with high amplitude but with changed frequency. Oscillations of clusters of yeast cells measured by Smith (16) were stopped if shunted by a DC leakage resistance of 10 MΩ. The leakage introduced by 10 MΩ was sufficient to upset the established conditions in cells. In our case the input impedance of the preamplifier may have represented a high load for the

Electromagn Biol Med Downloaded from informahealthcare.com by CDL-UC San Diego on 06/03/15
For personal use only.

Copyright © Marcel Dekker, Inc. All rights reserved.

Marcel Dekker, Inc.
270 Madison Avenue, New York, New York 10016

RIGHTSLINK

ORDER REPRINTS

low-power cellular sources and caused strong damping. If the measured signals are generated by the microtubule structures, the frequency jumps of the spectral lines may appear to have been due to treadmilling or dynamic instability. When a layer of tubulin heterodimers was added to or separated from a microtubule 2 μm long, the frequency shift of the vibration modes was of the order of 1–100 kHz as derived from analysis of the vibration modes in reference 6. For a growth rate of a kinetochore microtubule of 7 μm per 10 min (22), a frequency jump could happen within a time interval of about 1 sec. We did not observe unusual frequencies of the spectral lines on the printed records in the frequency range from 8–9 MHz. Spectral lines seem to be spread over this frequency band. Experimental

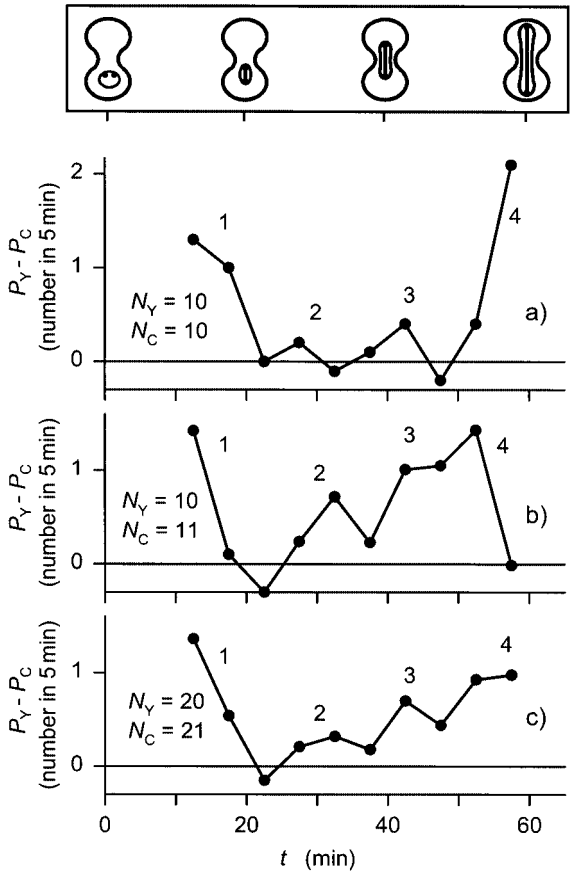


Figure 10. Difference of mean values of the number of evaluated spectral lines in 5-min subintervals of synchronized yeast cells and control experiments versus time t (groups 1 and 2). Measured values denoted by circles are connected with solid lines. Control experiment—sucrose: $P_Y - P_C$ for (a) group 1, (b) group 2, (c) groups 1 and 2. Control experiment—empty sensor: $P_Y - P_D$ for (d) group 1, (e) group 2, (f) groups 1 and 2. A schematic picture of the reassembly of microtubules is shown in the upper part of the figure.

(*continued*)

Electromagn Biol Med Downloaded from informahealthcare.com by CDL-UC San Diego on 06/03/15
For personal use only.

Copyright © Marcel Dekker, Inc. All rights reserved.

MARCEL DEKKER, INC.
270 Madison Avenue, New York, New York 10016

RIGHTSLINK

ORDER REPRINTS

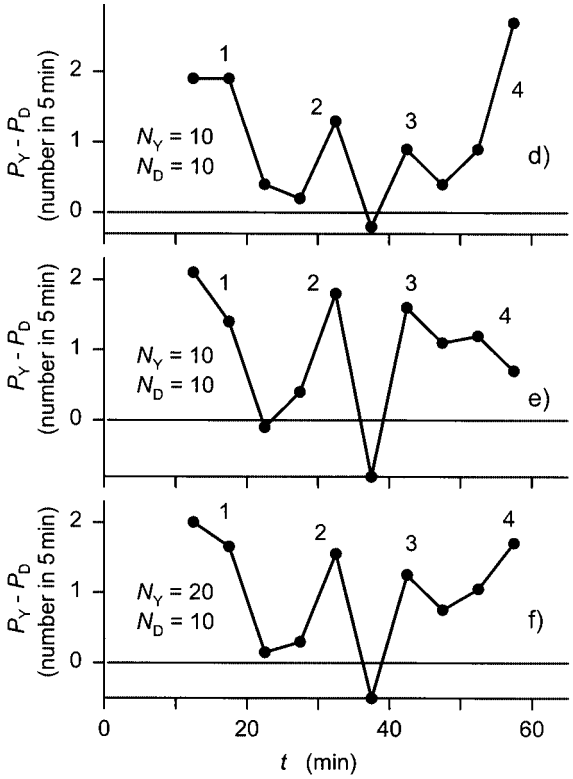


Figure 10. Continued.

analysis of the frequency dependence of the electromagnetic activity should be done over a wider frequency band, as follows from measurements described in references 16 and 17.

Groups 1 and 2

Figure 10a, b, c and d, e, f shows $P_Y - P_C$ (control group with sucrose) and $P_Y - P_D$ (control group with empty detector), respectively, versus time of synchronized yeast cells *tub2-401*. We used the microelectronic sensor (with a 4-μm gap between electrodes) (Fig. 10a, d) and alumina sensor (Fig. 10b, e). The spectrum analyzer ANR was used. Baseline data about the groups presented are listed in Table 1. The upper parts of Figure 10a, b, c and d, e, f show development of the microtubule spindle which served as a ''cellular clock'' (the same is shown in Figs. 11 and 12). The curves had four maxima that we arbitrarily describe as peaks 1, 2, 3, and 4. Peak 1 seems to coincide with formation of the mitotic spindle, peak 2 with the processes corresponding to late prometaphase and metaphase, peak 3 with anaphase A, and peak 4 with anaphase B. Small shifts of the position of peaks in Figure 10a and b may have been caused by noise fluctuations in the

Electromagn Biol Med Downloaded from informahealthcare.com by CDL-UC San Diego on 06/03/15
For personal use only.

Copyright © Marcel Dekker, Inc. All rights reserved.

MARCEL DEKKER, INC.
270 Madison Avenue, New York, New York 10016

RIGHTSLINK

ORDER REPRINTS

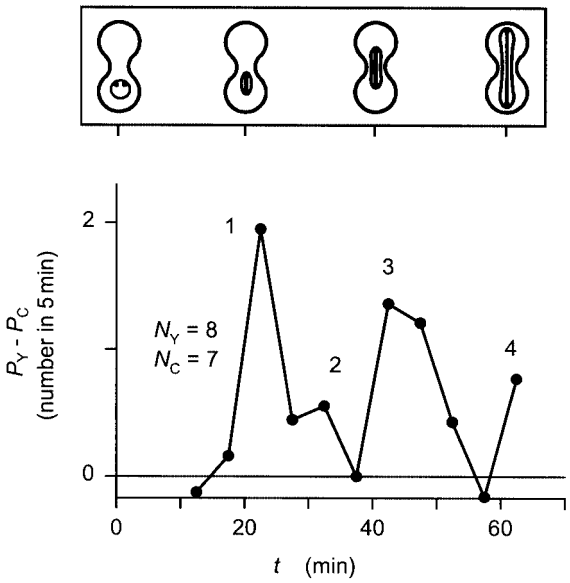


Figure 11. Difference of mean values of the number of evaluated spectral lines in 5 min subintervals of synchronized yeast cells and control experiments ($P_Y - P_C$) versus time t (group 3). Measured values denoted by circles are connected with solid lines. Control experiment—sucrose. A schematic picture of the reassembly of microtubules is shown in the upper part.

control measurements. Statistical evaluation is presented in Table 2. Only peaks 1 and 4 were statistically significant against control measurement with sucrose (Fig. 10c). All of the peaks were statistically significant versus control measurement with the empty detector (Fig. 10f). Peaks 1, 2, and 3 in Figure 10d and e coincided in time. Statistical assessment of hypotheses H1, H2, and H3 is listed in Table 3. None of the hypotheses was ruled out in group 2-C. Hypothesis H1 was ruled out in the groups 1-D, 2-D, 1,2-D, and hypothesis H2 was ruled out in groups 1-C, 1-D, 1,2-C (for $s \leq 0.05$) (Table 3).

Group 3

Figure 11 shows $P_Y - P_C$ versus time as measured with the alumina sensor. Spectrum analyzer R&S was used. The measured signal exhibited four peaks. Peak 1 is evidently shifted to greater values of time, which might have been caused by delay of the biological processes in the measured cells. Basic data about the group are shown in Table 1, and statistical significance is shown in Table 2. Peaks 1 and 3 were statistically significant ($s \leq 0.05$). Hypothesis H2 was ruled out as follows from Table 3 (for $s = 0.01$).

Electromagn Biol Med Downloaded from informahealthcare.com by CDL-UC San Diego on 06/03/15
For personal use only.

Copyright © Marcel Dekker, Inc. All rights reserved.

Marcel Dekker, Inc.
270 Madison Avenue, New York, New York 10016

RIGHTSLINK

ORDER REPRINTS

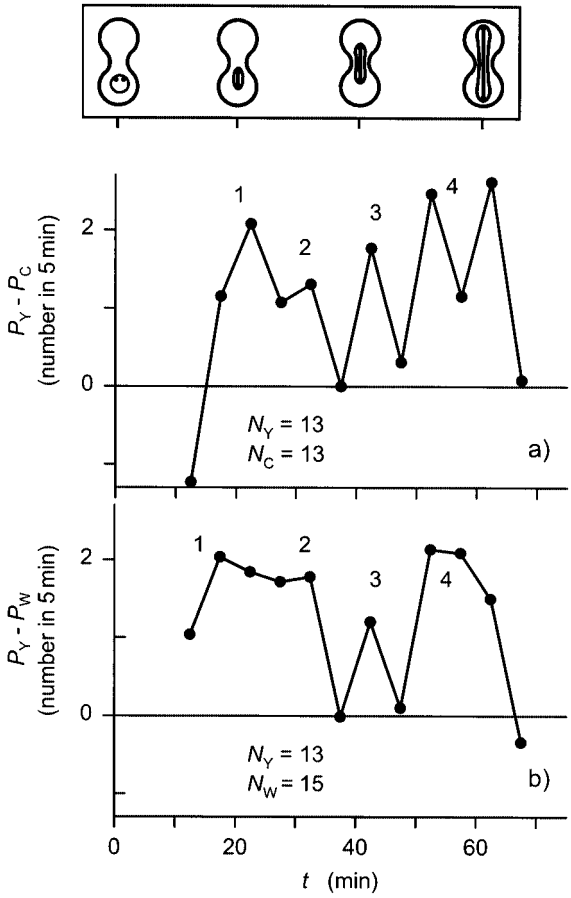


Figure 12. Difference of mean values of the number of evaluated spectral lines in 5-min subintervals of synchronized yeast cells and control experiments versus time (group 4). Measured values denoted by circles are connected with solid lines. Control experiment—sucrose: $P_Y - P_C$. Control experiment—wild strain of yeast cells: $P_Y - P_W$. A schematic picture of the reassembly of microtubules is shown in the upper part of the figure.

Group 4

Figure 12a, b shows $P_Y - P_C$ (the control experiment with sucrose) and $P_Y - P_W$ (the control experiments with a wild strain of yeast cells), respectively, versus time measured with a microelectronic sensor with a 7-μm gap between electrodes. Spectrum analyzer R&S was used. The peaks of the curves in Figure 12a, b were arbitrarily designated as 1, 2, 3, and 4. The shift of peak 1 in Figure 12a with respect to the same peak in Figure 12b was very likely caused by large fluctuations in the control measurement with sucrose. Peaks 1, 3, and 4 were statis-

Electromagn Biol Med Downloaded from informahealthcare.com by CDL-UC San Diego on 06/03/15
For personal use only.

Copyright © Marcel Dekker, Inc. All rights reserved.

Marcel Dekker, Inc.
270 Madison Avenue, New York, New York 10016

RIGHTSLINK

ORDER REPRINTS

Table 1. Overview of Experiments

Group	Cells	N_Y	N_c/N_W	Control	Figure
1-C	*tub2-401*	10	10	Sucrose	10a
2-C	*tub2-401*	10	11	Sucrose	10b
1,2-C	*tub2-401*	20	21	Sucrose	10c
1-D	*tub2-401*	10	10	Empty sensor	10d
2-D	*tub2-401*	10	10	Empty sensor	10e
1,2-D	*tub2-401*	20	10	Empty sensor	10f
3-C	*tub2-401*	8	7	Sucrose	11
4-C	*tub2-401*	13	13	Sucrose	12a
4-W	*tub2-401*	13	15	Nonsynchronized cells	12b
5-C	*tub2-406*	13	13	Sucrose	13a
5-W	*tub2-406*	13	13	Nonsynchronized cells	13b

Table 2. Statistical Evaluation: Values of the Test Statistic t and Significance Level s ($s = 0.1$ Indicated with ''—'')

		Time (min)											
Group (Figure)	Test Statistic	5− −10	10− −15	15− −20	20− −25	25− −30	30− −35	35− −40	40− −45	45− −50	50− −55	55− −60	60− −65
1-C (10a)	t		1.550									2.973	
	s		—									0.005	
2-C (10b)	t									1.532	1.698		
	s									—	—		
1,2-C (10c)	t		1.915								1.608	1.763	
	s		0.05								—	0.05	
1-D (10d)	t		2.752	2.317								3.806	
	s		0.01	0.025								0.005	
2-D (10e)	t		1.927	2.312			2.044		1.969	1.492	1.395		
	s		0.05	0.025			0.05		0.05	—	—		
1,2-D (10f)	t		3.126	2.916			1.820		2.097		1.517	2.509	
	s		0.005	0.005			0.05		0.025		—	0.01	
3-C (11)	t				2.963				1.860	3.104			
	s				0.01				0.05	0.005			
4-C (12a)	t				1.897		1.347		2.497		2.323		2.279
	s				0.05		—		0.01		0.025		0.025
4-W (12b)	t	1.575		2.373	1.691	2.220	1.708		1.925		2.216	2.772	
	s	—		0.025	—	0.025	0.05		0.05		0.025	0.01	
5-C (13a)	t	2.843	3.211	3.053	1.697				2.970	2.451	2.890		
	s	0.005	0.005	0.005	—				0.005	0.025	0.005		
5-W (13b)	t	2.380	2.685	1.997		1.461			1.696		2.523		
	s	0.025	0.01	0.05		—			—		0.01		

Electromagn Biol Med Downloaded from informahealthcare.com by CDL-UC San Diego on 06/03/15
For personal use only.

Copyright © Marcel Dekker, Inc. All rights reserved.

MARCEL DEKKER, INC.
270 Madison Avenue, New York, New York 10016

RIGHTSLINK

ORDER REPRINTS

Table 3. Significance Level s for H1, H2, and H3 Hypotheses ($s = 0.1$ Indicated with ''—'')

Group (Figure)	Basic Parameters N_2	C/D/W Y	$N_C/N_D/N_W$ N_Y	Mean	Statistical Results H1	H2	H3
1-C (10a)	11	C	10	2.848	0.2046	0.0234	0.7484
		Y	10	3.318		0.05	
2-C (10b)	11	C	11	2.752	0.2483	0.3004	0.8139
		Y	10	3.300			
1,2-C (10c)	11	C	21	2.797	0.0810	0.0017	0.8212
		Y	20	3.309	—	0.01	
1-D (10d)	11	D	10	2.318	0.0038	0.0070	0.2446
		Y	10	3.318	0.01	0.01	
2-D (10e)	11	D	10	2.318	0.0249	0.4187	0.1935
		Y	10	3.300	0.05		
1,2-D (10f)	11	D	10	2.318	0.0043	0.0563	0.2687
		Y	20	3.309	0.01	—	
3-C (11)	13	C	7	1.110	0.0573	0.0096	0.4535
		Y	8	1.635	—	0.01	
4-C (12a)	13	C	13	3.698	0.0671	0.0206	0.1184
		Y	13	4.722	—	0.05	
4-W (12b)	13	W	15	3.456	0.0078	0.2838	0.4218
		Y	13	4.722	0.01		
5-C (13a)	13	C	13	5.858	0.0052	0.3360	0.0631
		Y	13	8.598	0.01		—
5-W (13b)	13	W	13	6.473	0.0416	0.1558	0.3075
		Y	13	8.598	0.05		

tically significant (Table 2). The control measurement with nonsynchronized yeast cells is shown in Figure 12b. All four peaks were statistically significant (Table 2). Hypotheses H1 and H2 are ruled out in the groups 4-W and 4-C, respectively (for $s \leq 0.05$) (Table 3).

Group 5

Figure 13a, b shows $P_Y - P_C$ and $P_Y - P_W$ versus time for synchronous yeast cells *tub2-406*. Spectrum analyzer R&S was used. The time course of the curves in Figure 13a, b exhibited large maxima within the period 5–20 min from the beginning (statistical significance 0.01–0.005). Another maximum appeared at around 50 min (statistical significance 0.025–0.01). The first maximum coincided with depolymerization of nonfunctional microtubules; the second maximum coincided with polymerization and building up of functional microtubule structures. The time profiles of the curves of *tub2-406* (Fig. 13) differed from those of *tub2-401* (Figs. 10–12). Hypothesis H1 was ruled out in groups 5-W and 5-C (for $s \leq 0.05$) (Table 3).

Electromagn Biol Med Downloaded from informahealthcare.com by CDL-UC San Diego on 06/03/15
For personal use only.

Copyright © Marcel Dekker, Inc. All rights reserved.

MARCEL DEKKER, INC.
270 Madison Avenue, New York, New York 10016

RIGHTSLINK

ORDER REPRINTS

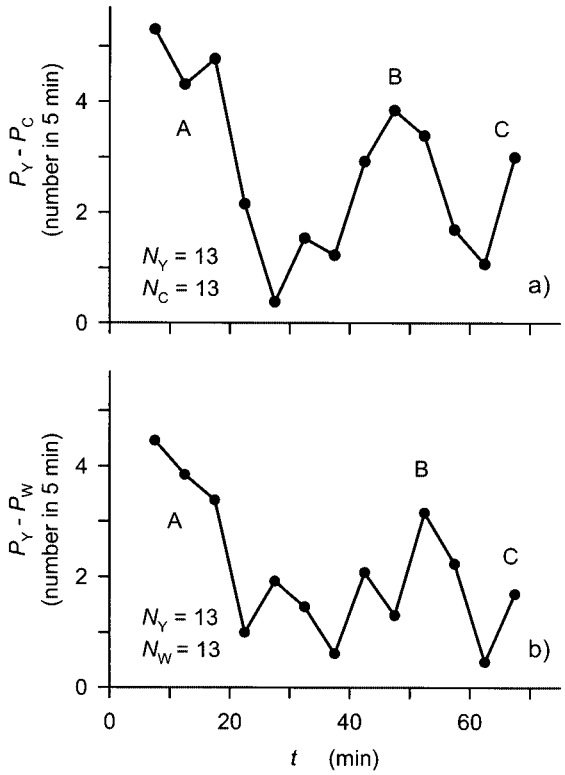


Figure 13. Difference of the mean values of the number of evaluated spectral lines in 5-min subintervals of synchronized yeast cells and control experiments versus time (group 5). Measured values denoted by circles are connected with solid lines. A, B, and C denote regions with high electromagnetic activity. Control experiment—sucrose: $P_Y - P_C$. Control experiment—wild strain of yeast cells: $P_Y - P_W$.

DISCUSSION

First, we will discuss compatibility of the technical equipment with requirements for measurement. The sensor and preamplifier had the greatest effect on the measured signal. Synchronized yeast cell groups and control groups were measured by different types of sensors: the sensor on a glass substrate (published in the previous paper, reference 19), a sensor on alumina substrate (Al_2O_3), and the microelectronic sensors on silicon substrates. The sensors had electrodes made of evaporated metal strips (Au), the width of which was 400 µm (sensors on glass and alumina substrates) or 10 µm (microelectronic sensors on silicon substrates). The gap between electrodes was 8 µm (glass and alumina substrates) and 4 and 7 µm (silicon substrates). Regardless of the sensors used, the measured signals did not differ substantially for the *tub2-401* cells. The time profiles of the measured signal in different groups had similar time dependencies within the M phase of the cell cycle. The preamplifier could influence the measured signal by reason of

Electromagn Biol Med Downloaded from informahealthcare.com by CDL-UC San Diego on 06/03/15
For personal use only.

Copyright © Marcel Dekker, Inc. All rights reserved.

Marcel Dekker, Inc.
270 Madison Avenue, New York, New York 10016

RIGHTSLINK

ORDER REPRINTS

the DC current in the input circuit. The effect of the DC current on yeast cells could be avoided by a capacitor separating the sensor from the input of the preamplifier. Positive feedback in the preamplifier could distort the measured signal. When we prepared the measurement system, we observed positive feedback in the preamplifier and took special care to avoid it.

We also analyzed the effects of control experiments. The control experiments were performed with empty sensors, with the suspending liquid (sucrose solution), and with a wild type of *S. cerevisiae* (nonsychronized yeast cells). The evaluated curves of $P_Y - P_D$, $P_Y - P_C$, and $P_Y - P_W$ did not depend on the type of control measurement. Control measurement with wild type of yeast cells is very likely the most convenient, because the experimental conditions equal those with synchronized cells (several layers of cells are at the bottom of the sensor cuvette). Noise fluctuations in the control measurement with sucrose solution seemed to be greater than those with an empty sensor, or with the wild strain of yeast cells, which may have resulted in a decrease in statistical significance, particularly if the voltage detected with the contacts of a sensor was small. This was very likely the case in 1-C and 2-C (Table 2). We used the microelectronic sensor with a 4-μm gap (which is about one-half of the linear cell dimension, and detected smaller voltages) for 1-C, and the alumina sensor with 400 μm width electrodes (with parallel leakage of detected signal) for 2-C.

Variations of the ambient temperature (27 ± 2°C) may have been too large, and caused variations of the rate of the M phase processes. Time between the preparation of cells and their measurement varied too. Control measurements with sucrose solution may also have been the source of fluctuations, because the conditions between contacts in a sensor differed from those with yeast cells (when several layers of cells were at the bottom and the suspending liquid could not flow freely).

We wanted to assess the possible source of the signal. We had to take into consideration that the signal may have been generated in the medium around the cells as well as inside the cells. In particular, we had to consider fluctuations of the membrane potential formed by ionic layers at both sides of the plasma membrane. Concentration of ions in a layer is about 0.2 M and the layer thickness is of the order of 1 nm. We roughly assessed fluctuations in the ionic charge layer around the cell (the ζ potential region) if the cell was placed in the gap between the electrodes (the widths of which are 10 μm) of the microelectronic sensor. The ζ potential region is between electrodes. Fluctuations of the charge caused fluctuations of the voltage in the input circuit. The volume of a layer 10 μm × 1 nm × 0.1 nm contains a charge of 10^{-17} C (i.e., about 100 elementary charges). If the capacity of the input circuit was 10 pF depletion, recharging of the layer caused voltage variations of about 10^{-6} V. For impedance of the input circuit 10^4 Ω, the corresponding power was 10^{-16} W. Nevertheless, the generated electric field had a strong effect on the charge fluctuations. We assume a mobility of ions $\mu = \sigma/N_i e \approx 5 \times 10^{-9} m^2/Vsec$, where $\sigma = 0.1$ S/m is the conductivity and N_i is the concentration of ions in 1 m^3. The diffusion coefficient $D = kT\mu/e$ is about

Electromagn Biol Med Downloaded from informahealthcare.com by CDL-UC San Diego on 06/03/15
For personal use only.

Copyright © Marcel Dekker, Inc. All rights reserved.

MARCEL DEKKER, INC.
270 Madison Avenue, New York, New York 10016

RIGHTSLINK

ORDER REPRINTS

$1.3 \times 10^{-10}\,m^2$/sec. The variance of the fluctuations in the time interval $t = 5 \times 10^{-8}$ sec (the frequency is 10^7 Hz) is $2Dt \approx 1.3 \times 10^{-17}\,m^2$ and its square root is about 3.6×10^{-9} m. In the same time interval the electric field with intensity of 10^8 V/m (generated by charge displacement) could have transported the ions to a distance of 10^{-8} m. Therefore, the depleted region caused by the fluctuations could have been recharged within a time interval shorter than one-half of the frequency period of the measured electromagnetic field. Still, we have to point out that the electromagnetic field generated inside the cell could have interacted with the ζ potential region and modulated the density of charge.

Vibrations in the membrane result in variations of its thickness. The frequency of these oscillations might have been much higher than frequencies in the measured band. The amplitude of these vibrations was very likely smaller than 1 nm. The cross-section of a lipid molecule (phospholipid or glycolipid) is of the order of 1 nm^2. The cross-sections of membrane proteins may be of the same order. As long as the vibrations were not coherent, they would hardly have caused measurable effects in the ionic layer.

Variations of the impedance of a cell represent variations of the impedance of the source in the input circuit of the preamplifier. The impedance of a cell may be altered, for instance, by penetration of water molecules in proteins or by formation of nonspecific pores in the plasma membrane (23) (the critical radius of nonspecific pores is about 10 nm, and their density may depend on conditions in the cell). The permitivity of water is about 30 times greater than the permitivity of lipids or proteins. Great changes of impedance may be caused by penetration of water molecules, but this mechanism may have been responsible for fluctuations only at considerably lower freqencies than in the band 8–9 MHz.

The supply of energy is an important feature for electromagnetic activity of living matter. Only the cellular structures with an energy supply can emit energy. We assume that one measured signal was connected with the biological activity of polar structures during mitosis. Such a structure is the mitotic spindle which consists of two spindle pole bodies and microtubules. In this respect, the participation of microtubules in controlling cellular processes and energy transformation has been described previously (24–27). Microtubules may accept energy through the mechanism of treadmilling and dynamic instability (10–12) and according to theoretical analysis, vibrations in microtubules may generate an electromagnetic field (6,28,29). We will assess the power that may be released from the mitotic spindle. The energy of a vibration mode was roughly assessed in reference 30. In the microtubules with a total length of 1 cm, energy from an excited mode (with the amplitude 0.5 nm) is of the order of 10^{-18} J. Other parts of cell may be excited together with microtubules (e.g., centrosomes, kinetochores, etc.) and total vibration energy may be considerably greater. If the energy 10^{-18} J is emitted from the microtubule in 0.1 sec, the power is 10^{-17} W. This value corresponds to the power of our measured signals.

After evaluation of the previous experiments published in reference 19, we

Electromagn Biol Med Downloaded from informahealthcare.com by CDL-UC San Diego on 06/03/15
For personal use only.

Copyright © Marcel Dekker, Inc. All rights reserved.

MARCEL DEKKER, INC.
270 Madison Avenue, New York, New York 10016

RIGHTSLINK

ORDER REPRINTS

assumed that electromagnetic activity was concentrated mainly in two regions on the time scale: the first corresponded to the metaphase stage and the second corresponded to anaphase B. Further experimental findings that we have presented in this paper enabled us to distinguish more detailed features of the electromagnetic activity. The electromagnetic activity seemed to coincide with development of the microtubule structures in the yeast cells during the M phase.

Synchronized mutants may release secondary messengers such as ions, radicals, and various small molecules whose concentration and activity maxima might correspond to particular stages in mitosis. This might have had an effect on our measured data. An essential difference was found between the time courses of electromagnetic activity of mutants *tub2-406* and *tub2-401*. Mutant *tub2-406* had high electromagnetic activity from the beginning of measurement (when nonfunctional microtubules are depolymerized; see Fig. 13), whereas activity of the mutant *tub2-401* increased from the beginning and reached a maximum value at about 15–25 min (when microtubules were being polymerized; see Fig. 12). Depolymerization is a fast event in comparison with nucleation and polymerization of microtubules. This suggests that the electromagnetic activity we saw might have been connected with microtubular dynamics.

The values of the statistical significance of particular peaks in different experiments differed. The measured signal was about 10^{-17} W, and was only slightly greater than noise. A greater number of experiments should be performed under precisely the same conditions to study the fine details of electromagnetic activity and to reduce the effect of noise. Hypothesis H3 is not ruled out in any group presented in this paper (but it was ruled out in the experiment presented in reference 19). We have to mention that the time dependence of P_Y measured in synchronous yeast cells differed from a similar dependence of P_C, P_D, or P_W of control measurements only in some time intervals. This fact might have had a large impact on the statistical assessment of the hypotheses H1, H2, and H3. The time shifts of particular peaks and variations of their amplitudes might have been caused by different biological properties of the measured cells, by temperature variations, or by noise. Investigations in the future should focus on finding the source of the emission and on examination of the effects of various ambient conditions, especially the effects of external chemical and physical agents.

Our experimental results support the idea that an electromagnetic field can be generated around yeast cells. We also would like to assess coherence of the field. The measured spectral lines were narrow. The resolution and the video bandwidth of the spectrum analyzers were 300 Hz and, therefore, the widths of the spectral lines are equal to or smaller than this value. Because the frequency of the measured signals was about 10^7 Hz, the relative width of a spectral line was about 10^{-4}–10^{-5}. Nevertheless, because of the transient character of the signal, the Fröhlich concept of coherent vibrations remains an open question. We would like to point out that other methods might be used to prove coherence of vibrations in cellular structures [e.g., a method based on the Mössbauer effect (31)].

Electromagn Biol Med Downloaded from informahealthcare.com by CDL-UC San Diego on 06/03/15
For personal use only.

Copyright © Marcel Dekker, Inc. All rights reserved.

Marcel Dekker, Inc.
270 Madison Avenue, New York, New York 10016

RIGHTSLINK

ORDER REPRINTS

CONCLUSIONS

Electromagnetic activity was measured in the vicinity of synchronized yeast cells during mitosis (cold-sensitive mutants *tub2-401* and *tub2-406* were used). This is an experimental system which is very suitable for continuous measurement of electromagnetic activity in cells synchronized in mitosis. After the mutant *tub2-401* was warmed from the restrictive to the permissive temperature, microtubules reassembled and the cells re-entered mitosis. Our experiments showed that the measured activity was associated with mitosis. Because the two arrested tubulin mutants, *tub2-401* and *tub2-406*, displayed different activity levels at the beginning of measurement, we suggest that the higher activity we observed was related to aberrant microtubules detected in the arrested *tub2-406* mutant. We suggest that four time periods of higher activity in the recovering *tub2-401* mutant seemed to coincide with the rearrangement of the microtubules into a mitotic spindle, with binding of chromatids to kinetochore microtubules, and with the elongation of mitotic spindles during anaphase A and B.

Pohl explained the attraction of small dielectric particles to yeast cells in the M phase of the cell cycle by dielectrophoretic effects. Experimental data presented in this paper support Pohl's idea of the existence of an electromagnetic field around yeast cells.

ACKNOWLEDGMENTS

This work was supported in part under Grant No. 102/97/0867 of the Grant Agency of the Czech Republic, and under Grant No. OC 244B.40 of Ministry of Education, Youth, and Sports of the Czech Republic in the framework of COST 244bis.

REFERENCES

1. Frauenfelder, H.; Wolynes, P.G.; Austin, R.H. Biological Physics. Reviews of Modern Physics **1999**, *71* (2), Centenary 1999, S419–S430.
2. Fröhlich, H. Quantum Mechanical Concepts in Biology. In *Theoretical Physics and Biology*; Marois, M., Ed.; North-Holland: Amsterdam, 1969; 13–22.
3. Fröhlich, H. Bose Condensation of Strongly Excited Longitudinal Electric Modes. Phys. Lett. **1968**, *26A*, 402–403.
4. Fröhlich, H. Long-Range Coherence and Energy Storage in Biological Systems. Int. J. Quant. Chem. **1968**, *II*, 641–649.
5. Fröhlich, H. The Biological Effects of Microwaves and Related Questions. Adv. Electronics Electron Phys. **1990**, *53*, 85–152.
6. Pokorný, J.; Wu, T.-M. *Biophysical Aspects of Coherence and Biological Order*; Academia: Prague; Springer: Berlin, 1998.

Electromagn Biol Med Downloaded from informahealthcare.com by CDL-UC San Diego on 06/03/15
For personal use only.

Copyright © Marcel Dekker, Inc. All rights reserved.

Marcel Dekker, Inc.
270 Madison Avenue, New York, New York 10016

RIGHTSLINK

ORDER REPRINTS

7. Pokorný, J. Conditions for Coherent Vibrations in the Cytoskeleton. Bioelectrochem. Bioenerg. **1999**, *48*, 267–271.
8. Pohl, H.A. Oscillating Fields About Growing Cells. Int. J. Quant. Chem. Quant. Biol. Symp. **1980**, *7*, 411–431.
9. Pohl, H.A.; Braden, T.; Robinson, S.; Piclardi, J.; Pohl, D.G. Life Cycle Alterations of the Micro-Dielectrophoretic Effects of Cells. J. Biol. Phys. **1981**, *9*, 133–154.
10. Caplow, M.; Ruhlen, R.L.; Shanks, J. The Free Energy for Hydrolysis of a Microtubule-Bound Nucleotide Triphosphate Is Near Zero: All of the Free Energy for Hydrolysis Is Stored in the Microtubule Lattice. J. Cell Biol. **1994**, *127*, 779–788.
11. Caplow, M.; Shanks, J. Induction of Microtubule Catastrophe by Formation of Tubulin–GDP and Apotubulin Subunits at Microtubule Ends. Biochem. **1995**, *34*, 15732–15741.
12. Caplow, M.; Shanks, J. Evidence that a Single Monolayer Tubulin–GTP Cap Is Both Necessary and Sufficient to Stabilize Microtubules. Molec. Biol. Cell **1996**, *7*, 663–675.
13. Rowlands, S.; Sewchand, L.S. A Quantum Mechanical Interaction of Human Erythrocytes. Canad. J. Physiol. Pharmacol. **1982**, *60*, 52–59.
14. Albrecht-Buehler, G. Rudimentary Form of Cellular 'Vision'. Proc. Natl. Acad. Sci. U.S.A. **1992**, *89*, 8288–8292.
15. Vos, M.H.; Rappaport, J.; Lambry, J.Ch.; Breton, J.; Martin, J.L. Visualization of Coherent Nuclear Motion in a Membrane Protein by Femtosecond Spectroscopy. Nature **1993**, *363*, 320–325.
16. Del Giudice, E.; Doglia, S.; Milani, M.; Smith, C.W.; Vitiello, G. Magnetic Flux Quantization and Josephson Behaviour in Living Systems. Phys. Scr. **1989**, *40*, 786–791.
17. Hölzel, R.; Lamprecht, I. Electromagnetic Field Around Biological Cells. Neural Network World **1994**, *4*, 327–337.
18. Jelínek, F.; Šaroch, J.; Trkal, V.; Pokorný, J. Measurement System for Experimental Verification of Fröhlich Electromagnetic Field. Bioelectrochem. Bioenerg. **1996**, *41*, 35–38.
19. Jelínek, F.; Pokorný, J.; Šaroch., J.; Trkal, V.; Hašek, J.; Palán, B. Microelectronic Sensors for Measurement of Electromagnetic Fields of Living Cells and Experimental Results. Bioelectrochem. Bioenerg. **1999**, *48*, 261–266.
20. Huffaker, T.C.; Thomas, J.H.; Botstein, D. Diverse Effects of β-Tubulin on Microtubule Formation and Function. J. Cell Biol. **1998**, *106*, 1997–2010.
21. Hašek, J.; Streiblová, E. Fluorescence Microscopy Methods. In *Methods in Molecular Biology*, *Vol. 53*: *Yeast Protocols*; Evans, I., Ed.; Humana Press: Totowa NJ, 1996; *53*, 392–405.
22. Hyman, A.A.; Mitchison, T.J. Modulation of Microtubule Stability by Kinetochores In Vitro. J. Cell Biol. **1990**, *110*, 1607–1616.
23. Litster, J.D. Stability of Lipid Bilayers and Red Blood Cell Membranes. Phys. Lett. **1975**, *53A*, 193–194.
24. Satarić, M.V.; Tuszyński J.A.; Žakula, R.B. Kinklike Excitations as an Energy-Transfer Mechanism in Microtubules. Phys. Rev. **1993**, *E 48*, 589–597.
25. Satarić, M.V.; Tuszyński, J.A.; Hameroff, S.; Žakula, R.B. Microtubules and Their Role in Neuromolecular Computing. Neural Network World **1994**, *4*, 281–294.
26. Tuszyński, J.A.; Hameroff, S.; Satarić, M.V.; Trpisová B.; Nip, M.L.A. Ferroelectric

Electromagn Biol Med Downloaded from informahealthcare.com by CDL-UC San Diego on 06/03/15
For personal use only.

Copyright © Marcel Dekker, Inc. All rights reserved.

MARCEL DEKKER, INC.
270 Madison Avenue, New York, New York 10016

RIGHTSLINK

ORDER REPRINTS

Behavior in Microtubule Dipole Lattices: Implications for Information Processing, Signaling and Assembly/Disassembly. J. Theor. Biol. **1995**, *174*, 371–380.
27. Tuszyński, J.A.; Trpisová, B.; Sept, D. From Erratic to Coherent Behaviour in the Assembly of Microtubules. Neural Network World **1995**, *5*, 675–688.
28. Pokorný, J.; Jelínek, F.; Trkal, V.; Lamprecht, I.; Hölzel, R. Vibrations in Microtubules. J. Biol. Phys. **1997**, *23*, 171–179.
29. Pokorný, J.; Jelínek, F.; Trkal, V. Electric Field Around Microtubules. Bioelectrochem. Bioenerg. **1998**, *45*, 239–245.
30. Pokorný, J.; Hašek, J.; Jelínek, F.; Šaroch, J.; Palán, B. *Electromagnetic Field Generated by Microtubules and Electromagnetic Field Around Yeast Cells*, Workshop Risk Assessment of Electromagnetic Pollution from Mobile Phone Networks, Varenna, Italy, May 10, 2000.
31. Satarić, M.V.; Zeković, S.; Tuszyński, J.A.; Pokorný, J. Mössbauer Effect as a Possible Tool in Detecting Nonlinear Excitations in Microtubules. Phys. Rev. **1998**, *E 58*, 6333–6339.

Electromagn Biol Med Downloaded from informahealthcare.com by CDL-UC San Diego on 06/03/15
For personal use only.

Copyright © Marcel Dekker, Inc. All rights reserved.

Marcel Dekker, Inc.
270 Madison Avenue, New York, New York 10016

RIGHTSLINK

Electromagn Biol Med Downloaded from informahealthcare.com by CDL-UC San Diego on 06/03/15
For personal use only.

Request Permission or Order Reprints Instantly!

Interested in copying and sharing this article? In most cases, U.S. Copyright Law requires that you get permission from the article's rightsholder before using copyrighted content.

All information and materials found in this article, including but not limited to text, trademarks, patents, logos, graphics and images (the "Materials"), are the copyrighted works and other forms of intellectual property of Marcel Dekker, Inc., or its licensors. All rights not expressly granted are reserved.

Get permission to lawfully reproduce and distribute the Materials or order reprints quickly and painlessly. Simply click on the "Request Permission/Reprints Here" link below and follow the instructions. Visit the U.S. Copyright Office for information on Fair Use limitations of U.S. copyright law. Please refer to The Association of American Publishers' (AAP) website for guidelines on Fair Use in the Classroom.

The Materials are for your personal use only and cannot be reformatted, reposted, resold or distributed by electronic means or otherwise without permission from Marcel Dekker, Inc. Marcel Dekker, Inc. grants you the limited right to display the Materials only on your personal computer or personal wireless device, and to copy and download single copies of such Materials provided that any copyright, trademark or other notice appearing on such Materials is also retained by, displayed, copied or downloaded as part of the Materials and is not removed or obscured, and provided you do not edit, modify, alter or enhance the Materials. Please refer to our Website User Agreement for more details.

Order now!

Reprints of this article can also be ordered at
http://www.dekker.com/servlet/product/DOI/101081JBC100108577

RIGHTSLINK